Option 1: **Geographic distribution of feather sulphur isotope compositions in Europe**

Option 2: **Geographic distribution of feather $\delta^{34}S$ in Europe**

Vojtěch Brlík[1,2], Petr Procházka[2], Luana Bontempo[3], Federica Camin[3,4,5], Frédéric Jiguet[6], Gergely Osváth[7,8], Craig A. Stricker[9], Michael B. Wunder[10,*], Rebecca L. Powell[11,*]

*these authors contributed equally

[1]Department of Ecology, Charles University, Prague, Czech Republic
[2]Czech Academy of Sciences, Institute of Vertebrate Biology, Brno, Czech Republic
[3]Traceability Unit, Research and Innovation Centre, Fondazione Edmund Mach, Trento, Italy
[4]Center Agriculture Food Environment (C3A), University of Trento, Via E. Mach, 1 - 38010 38098 San Michele all'Adige (TN), Italy
[5]International Atomic Energy Agency, Vienna International Centre, PO Box 100, A-1400 Vienna, Austria
[6]Museum National d'Histoire Naturelle, UMR7204 CESCO, Paris, France
[7]Musem of Zoology, Babeș-Bolyai University, Cluj-Napoca, Romania
[8]Evolutionary Ecology Group, Hungarian Department of Biology and Ecology, Babeș-Bolyai University, Cluj-Napoca, Romania
[9]United States Geological Survey, Denver Federal Center, Denver, USA
[10]University of Colorado Denver, Department of Integrative Biology, Denver, USA
[11]University of Denver, Department of Geography and the Environment, Denver, USA

VB – https://orcid.org/0000-0002-7902-8123
PP – https://orcid.org/0000-0001-9385-4547
LB – https://orcid.org/0000-0001-7583-1501
FJ – https://orcid.org/0000-0002-0606-7332
GO – https://orcid.org/0000-0003-1542-9128
CAS – https://orcid.org/000-0002-5031-9437
MBW – https://orcid.org/0000-0002-8063-2408
RLP – https://orcid.org/0000-0002-1978-0153

Abstract

Geographic distribution maps of environmental stable isotopes (so called 'isoscapes') are widely applied in animal ecology, wildlife forensics and conservation. However, the application of these isoscapes is limited to elements and regions for which the spatial patterns are known. Here, we focused on less commonly used yet ubiquitous stable sulphur isotope (^{34}S). To predict the European $\delta^{34}S$ isoscape, we used 242 feather samples from Eurasian Reed Warbler (*Acrocephalus scirpaceus*) formed at 69 European wetland sites. We quantified the relationships between sample $\delta^{34}S$ and environmental covariates using random forest regression model and applied the model to predict the geographic distribution of $\delta^{34}S$. We also quantified within-site variation in $\delta^{34}S$ and complementarity of $\delta^{34}S$ with other isotopes on both individual and isoscape levels. The predicted feather $\delta^{34}S$ isoscape shows only slight differences between the central and southern parts of Europe while the coastal regions were most enriched in ^{34}S. The most important covariates of $\delta^{34}S$ were distance to coastline, surface elevation and atmospheric concentrations of SO_2 gases. The absence of a systematic spatial pattern impedes the application of the sole $\delta^{34}S$ isoscape but high complemetarity with other isoscapes advocates the combination of multiple isoscapes to increase precision of animal tracing. The feather $\delta^{34}S$ measures showed considerable within-site variation with highest values in inland parts of Europe and likely attibute to wetland anaerobic conditions and redox sensitivity of sulphur. The complex European geography and topography as well as using $\delta^{34}S$ samples from wetlands may contribute to the absence of a systematic spatial gradient of $\delta^{34}S$ values in Europe. We thus encourage future studies to focus on geographic distribution of $\delta^{34}S$ using tissues from diverse taxa collected in various habitats in geographically uniform parts of the world (i.e., Africa, South America or East Asia).

Introduction

Stable isotopic composition vary spatially due to a wide variety of biogeochemical processes (West et al. 2010). These geographic distributions of isotopes (i.e., 'isoscapes') can be used to infer spatial origin and have manifold applications, especially in animal ecology, wildlife forensics and conservation (Hobson and Wassenaar 2018). Isoscapes are used to infer geographic space use and thus applied to study altitudinal migration (Villegas et al. 2016), to quantify strength of migratory connectivity (Norris et al. 2006) or to trace natal origins of animals (Procházka et al. 2013). Geographic space use can affect animals and stable isotopes thus may indirectly inform demographic models to understand population changes and target conservation efforts (Jiguet et al. 2019). Continental-scale isoscapes essential for tracing origins are currently available for $\delta^{2}H$, $\delta^{13}C$, $\delta^{15}N$, $\delta^{18}O$ and $^{87}Sr/^{86}Sr$, but their application is limited to regions with steep isotopic gradients or isotopically-distinct regions (Amundson et al. 2003, West et al. 2010, Bataille et al. 2020).

Some continental and global isoscapes feature systematic spatial pattern on continental scales (e.g., $\delta^{2}H$ and $\delta^{18}O$ in North America and East Asia)(Bowen and Revenaugh 2003) while others show weak spatial structure (e.g., $\delta^{13}C$ and $\delta^{15}N$ in Africa and South America) (Amundson et al. 2003, Powell and Still 2010) limiting their application. Alternatively, the combination of spatial predictions using multiple isoscapes can be used to increase precision of tracing (e.g.,) (Popa-Lisseanu et al. 2012, Veen et al. 2014). Either way, developing isotopic maps is essential for broadening the potential of isotopes in animal ecology and wildlife forensics.

Geographic distributions of stable sulphur isotopes ($\delta^{34}S$) in recent organic tissues have already been modelled for Great Britain, Tanzania and the conterminous USA (Valenzuela et al. 2011, Kabalika et al. 2020, Newton 2021). Additionally, a recent study used archaeological remains

to predict geographic distribution of $\delta^{34}S$ in Europe (Bataille et al. 2021). Moreover, deposition of marine-derived sulphates from coastal towards inland areas was identified as the most important driver of $\delta^{34}S$ geographic distribution (Lott et al. 2003, Zazzo et al. 2011). Gradients formed by the deposition of marine sulphates have been detected on both regional (Wadleigh and Blake 1999, Zazzo et al. 2011) and continental scales (Valenzuela et al. 2011, Bataille et al. 2021). In addition, spatial variation in atmospheric concentrations of combustion gases and bedrock geochemistry, have also been found to affect spatial patterns of $\delta^{34}S$ values (Case and Krouse 1980, Thode 1991). Collectively, the detailed knowledge of these relationships could be used to predict $\delta^{34}S$ geographic distributions on continental scales. The isotopic offset between environment and tissue is generally low for $\delta^{34}S$ in organic tissues (Felicetti et al. 2003, McCutchan et al. 2003, Florin et al. 2011, Tcherkez and Tea 2013) providing an opportunity to apply a single $\delta^{34}S$ isoscape to a range of taxa. Despite these benefits, continental $\delta^{34}S$ isoscapes of organic tissues are currently available only for part of North America and for human archaeological remains in Europe (Valenzuela et al. 2011, Bataille et al. 2021).

In this study, we (i) develop a European $\delta^{34}S$ isoscape using feather keratin samples, (ii) quantify within-site variation in $\delta^{34}S$, and (iii) quantify complementarity of $\delta^{34}S$ with other isotopes on individual and isoscape levels.

Methods

Sample collection

We used 242 feathers from Eurasian Reed Warbler (*Acrocephalus scirpaceus*) with known geographic origin at 69 European wetland sites previously used in Procházka et al. (2013) and newly collected in 2019 (Fig 1). At these sites, we collected the innermost primary feathers from one to four juvenile Eurasian Reed Warblers (one sample = 8 sites; two = 2; three = 6 and four = 53) during the fledgling period (June-early August; Fig 1). Juveniles of the Eurasian Reed Warbler are mostly stationary during this period before post-fledging dispersal (Mukhin 2004, Grinkevich et al. 2009) and we consider the sampling locations their natal origins and thus geographic origins of these samples.

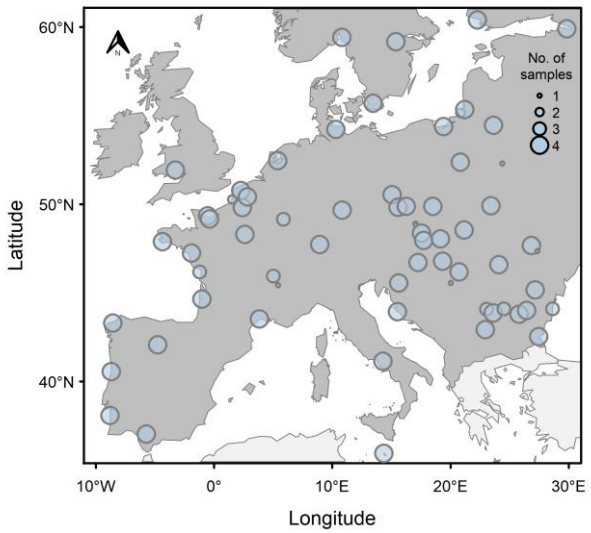


*Fig 1: Locations of European sampling sites (n = 69) coinciding with the geographic origins of feather samples collected from Eurasian Reed Warblers (*Acrocephalus scirpaceus*; n = 242). Dark grey region depicts the extent of prediction.*

Isotopic analysis

We cleaned the feather samples in a 2:1 chloroform:methanol mixture to remove surface lipids and other contaminants, and air dried the samples. Feather vane material of about 300 µg encapsulated in tin capsules was then combusted using a Vario Isotope Cube Elementar Ananlyser (Elementar Analysensysteme GmbH, Germany). Resulting SO_2, CO_2 and N_2 gases were transferred to isotope ratio mass spectrometer (VisIon, Elementar Analysensysteme GmbH) via a continuous flow-through inlet system. Sample $^{34}S/^{32}S$, $^{13}C/^{12}C$ and $^{15}N/^{14}N$ ratios are expressed in the delta notations ($\delta^{34}S$, $\delta^{13}C$ and $\delta^{15}N$) in parts per mil (‰) and relative to the following standards V-PDB (Vienna-Pee Dee Belemnite) for $\delta^{13}C$, Air for $\delta^{15}N$, V-CDT (Vienna-Canyon Diablo Troilite) for $\delta^{34}S$ according to:

$$\delta^{i}E = \frac{{}^{i}R_{sample} - {}^{i}R_{standard}}{{}^{i}R_{standard}}$$

where the superscript *i* indicates the mass number of the heavier isotope of element *E* (*e.g.*, ^{34}S) and *R* the isotope ratio of *E* (*e.g.*, $^{34}S/^{32}S$) in the sample and in the internationally recognized standard. Values of $\delta^{34}S$, $\delta^{13}C$ and $\delta^{15}N$ were calculated against working in-house standards which were themselves calibrated against international reference materials using multi-point normalisation: fuel oil NBS-22 (IAEA International Atomic Energy Agency, Vienna, Austria;−30.03 ‰) and sugar IAEA-CH-6 (−10.45 ‰) for $\delta^{13}C$, L-glutamic acid USGS 40 (−26.39 ‰ and−4.5 ‰ for $\delta^{13}C$ and $\delta^{15}N$), hair USGS 42 ($\delta^{15}N$ = +8.05 ‰, $\delta^{13}C$ = −21.09 ‰ and $\delta^{34}S$ = +7.84 ± 0.25 ‰) and USGS 43 ($\delta^{15}N$ = +8.44 ‰, $\delta^{13}C$ = −21.28 ‰ and $\delta^{34}S$ = +10.46 ± 0.22‰) for $^{13}C/^{12}C$, $^{15}N/^{14}N$ and $^{34}S/^{32}S$, barium sulphates IAEA-SO-5 and NBS 127 (IAEA) for $^{34}S/^{32}S$. Values of $\delta^{13}C$ were expressed versus V-PDB on a scale normalised against the two reference materials LSVEC (−46.6 ‰) and NBS 19 (+1.95 ‰). Values of $\delta^{15}N$ were expressed versus Air-N_2 on a scale normalised using two reference materials, IAEA-N-1 and USGS32, with consensus values of +0.4 ‰ and +180 ‰. Each sample was analysed three times and we present its isotopic composition as an average value. Measurement error, calculated as one standard deviation of internal laboratory standard measured ten times, for $\delta^{34}S$ was ± 0.4‰; for $\delta^{13}C$ was ± 0.1‰ and for $\delta^{15}N$ was ± 0.2‰. Stable isotope analysis was conducted in the Traceability Unit at the Research and Innovation Centre, Fondazione Edmund Mach, Italy.

Covariates of $\delta^{34}S$

We gathered geographic distributions of potential atmospheric, anthropogenic, geographical and geological covariates of $\delta^{34}S$ values, including SO_2 atmospheric concentrations (Case and Krouse 1980, Ohizumi and Fukuzaki 1997), distance to coastline (Valenzuela et al. 2011, Zazzo et al. 2011), and bedrock age and type (Thode et al. 1953, Case and Krouse 1980). Moreover, we extracted the geographic distribution of NO_2 atmospheric concentrations – tracing the intensity of various-source combustion – and log human population density, which affects the intensity of fossil fuel combustion (Garg et al. 2001, Martin et al. 2003). We also included surface elevation as a covariate, as we expected depletion in ^{34}S with increasing elevation (atmospheric deposition), similar to the patterns observed in water isotopes (Dansgaard 1954, 1964). The original spatial resolution and sources of covariate distribution layers are detailed in Table 1. Geographic distribution layers were gathered using a cloud-based geospatial analysis platform Google Earth Engine (Gorelick et al. 2017).

Table 1: Covariates used for modelling the geographic distribution of feather $\delta^{34}S$ values from Eurasian Reed Warblers (Acrocephalus scirpaceus) across Europe.

Covariate	*Units*	*Year*	*Original resolution*	*Source*
SO_2 atmospheric concentration	mol m^{-2}	2018	1 km	(Copernicus Sentinel 2015a)
NO_2 atmospheric concentration	mol m^{-2}	2018	1 km	(Copernicus Sentinel 2015b)
Human density	log persons km^{-2}	2010	0.8 km	(CIESIN 2018)
Distance to coastline	km	-	1 km	(NASA Ocean Biology Processing Group 2012)
Surface elevation	m a.s.l.	-	0.8 km	(Danielson and Gesch 2011)
Bedrock type*	nominal (class)	-	discrete	(Pawlewicz et al. 2003)
Bedrock age*	nominal (years)	-	discrete	(Pawlewicz et al. 2003)

**Layers were derived from vector layers with scale of 1:5000000.*

Geostatistical analysis

We resampled the spatial resolution of all covariate layers at 2 km to match scale of potential within-natal site movements of juvenile Eurasian Reed Warblers and extracted covariate values for each sample at each sampling location. We calculated average $\delta^{34}S$ values at sampling sites (or took a single measurement) for further analysis (n = 69). To identify and quantify relationships between covariates and average feather $\delta^{34}S$ at the sites, we employed a random forest regression model using the R package caret (Kuhn 2008). Random forest models are based on a large number of regression trees grown using a randomly sampled subset of the training dataset (Breiman 2001, Belgiu and Dragut 2016). Random forest models can accommodate different data types including e.g., categorical covariates. This enables to predict abrupt changes in the spatial surfaces by avoiding smoothing over the regions (Bataille et al. 2018, 2021). We built the random forest model with 500 regression trees, randomly selecting two covariates at each node, and estimating model accuracy using leave-one-out cross-validation. In this process, each observation was withheld for subsequent validation of an entire random forest model, and this process was repeated for each observation (Vapnik 1998). We derived the relative importance of individual covariates (index of node purity) and visualised the partial dependencies (relationships) of these covariates on $\delta^{34}S$. We then applied the final random forest regression model to covariate values per grid cell and predicted the geographic distribution of feather $\delta^{34}S$ values within the extent of prediction (Fig 2). We present the predicted $\delta^{34}S$ isoscape for Europe <31°N, <61°N without Greece and Turkey, and for elevations up to 750 m a.s.l. These restrictions reflect the geographic range of sampling sites and their upper range of elevations (Fig 1).

Similarly, we quantified the relationships between the within-site standard deviation of $\delta^{34}S$ values and the covariates. We calculated witin-site standard deviation for each sampling site with at least three $\delta^{34}S$ values (total of 230 samples from 59 sites) and employed the random forest regression model as detailed above. Finally, we quantified the relationship between average within-site $\delta^{34}S$ values and within-site standard deviations of $\delta^{34}S$ values using Pearson's correlation coefficients.

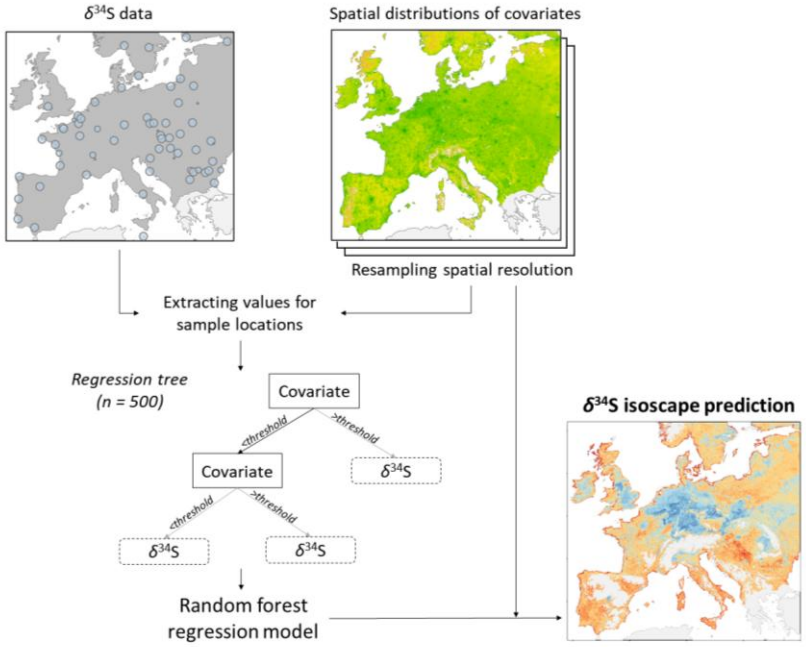


Fig 2. Flowchart showing the process of deriving the European feather $\delta^{34}S$ isoscape. Dots in the map depict the geographic origin of samples used to derive the $\delta^{34}S$ isoscape (n = 69). See Methods for more details.

Complementarity of $\delta^{34}S$ with other isotopes

We quantified the individual-level complementarity of isotope measures in feather samples using Pearson's correlation coefficient. We correlated the feather $\delta^{34}S$ values with the feather $\delta^{13}C$ and $\delta^{15}N$ values measured in Eurasian Reed Warblers (n = 242). Similarly, we assessed the isoscape-level complementarity to identify similarities among spatial patterns of isoscapes. We compared spatial patterns using per-grid-cell Pearson's correlation coefficients between the predicted $\delta^{34}S$ isoscape and the previously known feather-based $\delta^{2}H$ and $\delta^{13}C$ isoscapes. At both individual and isoscape levels low correlations indicate high level of complementarity.

For this purpose, we prepared the European feather $\delta^{2}H$ isoscape. We extracted $\delta^{2}H$ in precipitation from Global Network of Isotopes in Precipitation and applied a geospatial model to predict the $\delta^{2}H$ isoscape using precipitation, average temperature, surface elevation, absolute latitude as independent explanatory variables via a web-based computing platform IsoMAP (Bowen et al. 2014) (task key: 84119). We calibrated the resulting isoscape of $\delta^{2}H$ in precipitation using the equation $\delta^{2}H_{feather} = 1.28 \times \delta^{2}H_{precipitation} - 10.29$ to account for discrimination between precipitation and feather $\delta^{2}H$ in the Eurasian Reed Warbler derived by Procházka et al. (2013), and resampled to the spatial resolution the predicted feather $\delta^{34}S$ isoscape.

Similarly, we prepared the European plant $\delta^{13}C$ isoscape by combining climatic (Abatzoglou et al. 2018), land cover (Buchhorn et al. 2020) and crop production layers (Yu et al. 2020). We adapted process described in Powell et al. (2012) and Powell et al. (2019) using Google Earth Engine (Gorelick et al. 2017). We accounted for an assumed plant–feather discrimination by adding +2‰ to the plant $\delta^{13}C$ isoscape (Hobson et al. 2012) and resampled to the spatial resolution of the predicted feather $\delta^{34}S$ isoscape. Analyses were conducted in R 3.5.1 (R Core Team 2019).

Results

Geographic distribution of $\delta^{34}S$ and main covariates

The predicted feather $\delta^{34}S$ isoscape features a region depleted in ^{34}S over eastern Great Britain, Benelux, Germany, Poland, and northern Ukraine. In contrast, northern Europe (i.e., Norway, Denmark, Sweden, Finland, and Baltic states) and western to southern Europe (i.e., the Iberian Peninsula, France, Italy, the Balkans, Romania, and Bulgaria), together with European coastline were more enriched in ^{34}S (Fig 3).

The most important covariates of $\delta^{34}S$ values were distance to coastline, surface elevation, and atmospheric concentrations of SO_2 (Fig 4). The relationships between the covariates and the $\delta^{34}S$ values were i) negative (depletion in ^{34}S) for distance to coastline, surface elevation and human density, ii) positive (enrichment in ^{34}S) for bedrock age, and iii) more complex for atmospheric concentrations of SO_2 and NO_2 (Fig 4).

Overall, the random forest regression model explained 90% of the variance in the training dataset (predicted vs. observed values; slope = 1.5 [SE = 0.1], intercept = -0.4 [0.3]) and the cross-validation explained 15% of variance (slope = 0.8 [0.3], intercept = 0.4 [1.0]). Root mean square error of the final model was 6.1‰ representing 14% of the range of the $\delta^{34}S$ in the training dataset.

Within-site variation in $\delta^{34}S$

The average within-site variation (SD) in feather $\delta^{34}S$ was 2.1 ‰ (median = 1.3, min = 0.1, 1st quartile = 0.7, 3rd quartile = 2.5, max = 9.1). Overall, the highest within-site variation was detected in some inland parts of Europe (i.e., France, Germany, Hungary, southern Poland) while the lowest values appeared in coastal regions (Fig 5). The correlation between the within-site averages and within-site standard deviations was -0.21 [Pearson's correlation; 95% CI = -0.44; 0.05] and sites close to the coastline tended to show low within-site variability (ρ = 0.29 95% CI [0.05; 0.51]). The random forest regression model of within-site variability explained 87% of variance in the training dataset (slope = 2.3 [SE = 0.1], intercept = -2.2 [0.2]) but the cross-validation explained no variance (slope = 0.3 [SE = 0.4], intercept = 1.4 [SE = 0.9]). Root mean square error of the model was 1.6‰ representing 18% of the range of the values in the training dataset. Due to the low performance of the model, we did not predict the geographic distribution of within-site variability across Europe but present raw values only (Fig 5).

Complementarity of $\delta^{34}S$ with other isotopes

The feather $\delta^{34}S$ values ranged between -27.6 and 20.4‰ (mean = 1.0, SD = 8.5, n = 242), $\delta^{13}C$ values ranged between -28.9 and -11.5‰ (mean = -23.9, SD = 2.1, n = 242) and $\delta^{15}N$ values ranged between 6.5 and 25.6‰ (mean = 12.6, SD = 2.7, n = 242). The feather $\delta^{34}S$ values were weakly related to both $\delta^{13}C$ (ρ = 0.29; 95% CI [0.17; 0.40]) and $\delta^{15}N$ (ρ = -0.19; 95% CI [-0.30;-0.06]; Fig. 6). Similarly, we identified only weak relationships of the predicted feather European $\delta^{34}S$ isoscape with the feather $\delta^{2}H$ (ρ = 0.19) or feather $\delta^{13}C$ isoscapes (ρ = 0.01; Fig. 7).

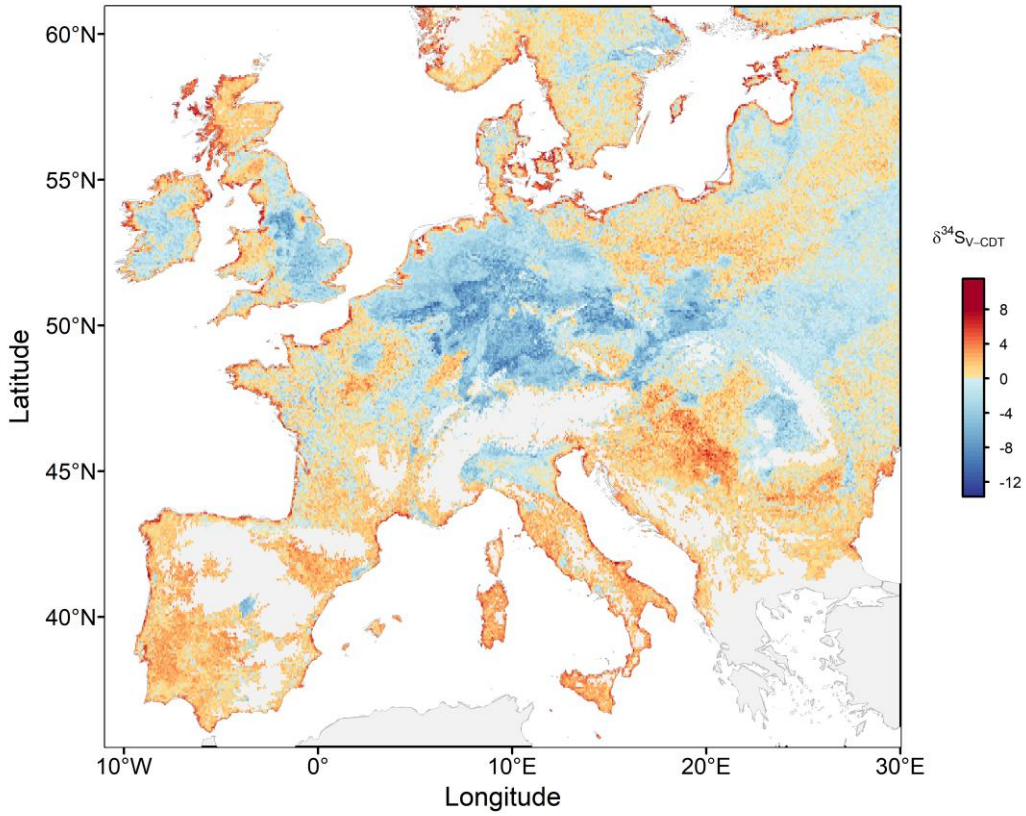


*Fig 3. The predicted geographic distribution of $\delta^{34}S$ values in Europe derived using Eurasian Reed Warbler (*Acrocephalus scirpaceus*) feather samples of known spatial origin, grey colour represents regions outside prediction range.*

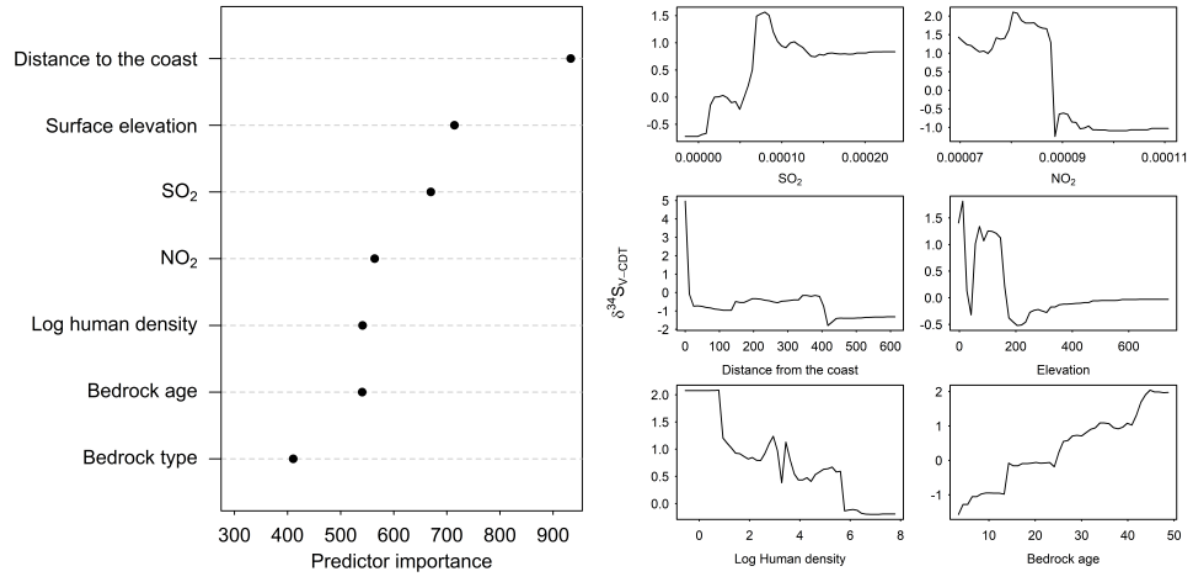


Fig 4. Relative importance of covariates (left) and partial dependencies of $\delta^{34}S$ on covariates (right).

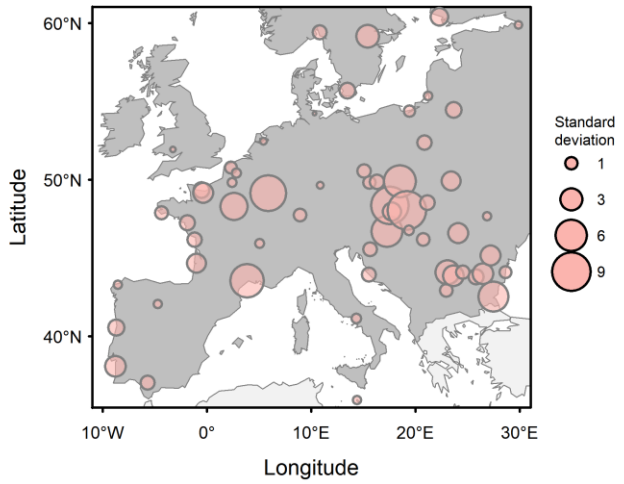


Fig 5: Within-site variability presented as standard deviation of feather $\delta^{34}S$ values at sampling sites with at least three collected samples (59 sites).

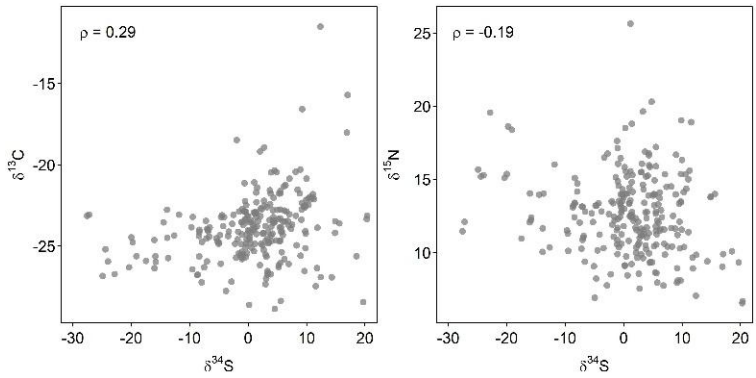


Fig 6: Relationship between feather $\delta^{34}S$ and $\delta^{13}C$ (left) and $\delta^{34}S$ and $\delta^{15}N$ (right) measurements (n = 242) including Pearson's correlation coefficients.

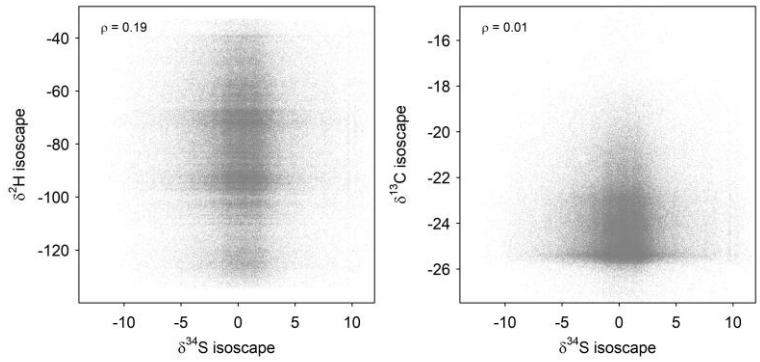


Fig 7: Relationships between the feather $\delta^{34}S$ and $\delta^{2}H$ isoscapes (left), and the feather $\delta^{34}S$ and $\delta^{13}C$ isoscapes (right) including Pearson's correlation coefficients.

Discussion

We predicted the geographic distribution of $\delta^{34}S$ values in Europe using feather samples of known geographical origin. The $\delta^{34}S$ isoscape shows high $\delta^{34}S$ values along the European coast and only slight differences in $\delta^{34}S$ values between the central and southern parts of Europe. The $\delta^{34}S$ values also varied highly within sites, especially, in inland parts of Europe. The absence of a systematic spatial pattern may limit the solitary use of the $\delta^{34}S$ isoscape but high complemetarity with other isoscapes advocates the combination of multiple isoscapes to increase precision of animal tracing.

Geographic distribution and main covariates of $\delta^{34}S$

Coastal regions being the most enriched in ^{34}S and the distance to coastline being a key covariate of the geographic distribution of $\delta^{34}S$ is in line with our predictions and previous studies (Fry 2006, Zazzo et al. 2011, Amrani et al. 2013). In contrast, the inland parts of Europe showed only slight differences in $\delta^{34}S$ values between the regions and the absence of a systematic spatial pattern thus contrasts with previous regional- and continental-scales assessments (Wadleigh and Blake 1999, Valenzuela et al. 2011, Bataille et al. 2021, Newton 2021). Among the explanations for the absence of such systematic spatial patterns in Europe could be: (i) the complex geography of the European continent, (ii) the spatial clustering of human population with related distribution of fossil fuel combustion intensity, and (iii) the effect of anaerobic conditions on tissue $\delta^{34}S$ isotopic composition in wetland environments.

The transportation of marine sulphate aerosols creates the coast-inland gradient of $\delta^{34}S$ values on regional and continental scales (Valenzuela et al. 2011, Zazzo et al. 2011). However, the European continent has complex coastal geography, intersected by mountain ranges, and contains regions with distinct climates (Beck et al. 2018) and variable patterns (Troen and Petersen 1989). Complex geography and wind systems could disrupt inland transportation of marine sulphates towards inland, partly explaining the patchiness of the predicted $\delta^{34}S$ isoscape. This explanation would be indirectly supported by the presence of a $\delta^{34}S$ gradient over homogeneous land masses in North America (Valenzuela et al. 2011) or differences between feather $\delta^{34}S$ values grown in central and western sub-Saharan Africa (Procházka et al. 2018). However, our explanation lacks direct support and contradicts the recent European $\delta^{34}S$ isoscape based on mostly archaeological remains and historical samples that shows a continent-wide coast-inland gradient of $\delta^{34}S$ values within Europe (Bataille et al. 2021).

Human populations have boomed in the past century as well as the intensity of anthropogenic activities. Human population growth has influenced atmospheric concentrations of combustion gases (i.e., SO_2 and NO_2) that we identified as important covariates of $\delta^{34}S$ values. Human population and related anthropogenic sources of these gases are, however, spatially clustered with numerous local peaks (e.g., in cities and around factories) with highest densities in central and western parts of Europe. A clustered geographic distribution of these covariates could further disrupt coast-inland gradient of $\delta^{34}S$ values caused by marine-derived sulphate aerosols (Rees et al. 1978, Zazzo et al. 2011) and result in patchiness of the predicted feather $\delta^{34}S$ isoscape.

Finally, the overall patchiness of the predicted feather $\delta^{34}S$ isoscape could be related to biological conditions in wetlands – the breeding habitat of the Eurasian Reed Warbler and the only habitat we sampled. Wetlands store water, and accumulate organic material and nutrients from surrounding areas. Consequently, geochemical conditions in the wetland may be affected by the catchment capacity of water reservoirs, collecting water leaching various bedrocks in the surrounding region (of uknown area). Moreover, high availability of nutrients and low oxygen levels support development of anaerobic conditions (Cherry 2011) and related bacterial comunities. These

bacteria affect $\delta^{34}S$ composition through fractionation against ^{34}S, resulting in substantial depletion in ^{34}S in solid-phase sulphur-bearing minerals such as pyrite (Chambers and Trudinger 1979, Thode 1991). Unfortunately, the anaerobic conditions in wetlands cannot be predicted from remote sensing imagery and are thus difficult to quantify on continental scales. Finally, the predicted feather $\delta^{34}S$ isoscape considers the relationships identified within wetland sampling sites but applies these relationships to predict $\delta^{34}S$ values over Europe potentially leading to bias (due to e.g., an absence of low redox conditions in terrestrial habitats).

Within-site variation in $\delta^{34}S$

We found large differences in within-site $\delta^{34}S$ variation with the highest values detected at some inland sites in Europe. In contrast, the coastal sites showed mostly low variation, which could be explained by the prevailing impact of marine-derived sulphates with uniform $\delta^{34}S$ values (Rees et al. 1978). Within-site variation in $\delta^{34}S$ also tended to increase with increasing distance to coastline likely due to reduced transport of marine sulphates and an increasing impact of low redox conditions in wetland environments (Chambers and Trudinger 1979, Thode 1991), which could vary locally both between patches within an individual wetland and regionally among wetlands.

Moreover, our measurements of within-site variability are based on three to four feather samples collected from juvenile Eurasian Reed Warblers during post-fledgling period at each site. The limited sample sizes could have contributed to large within-site variation due to stochasticity. Potential post-fledgling dispersals of juvenile Eurasian Reed Warblers between wetlands (Mukhin 2004) could further increase the variation detected at sampling sites. Similarly, the fledglings could opportunistically use food resources within the wetland as well as in the surrounding terrestrial habitats with different isotopic signatures adding to the within-site variation in $\delta^{34}S$. The high within-site variation thus largely limits the effective use of the predicted feather $\delta^{34}S$ isoscape for animal tracing in Europe.

Complementarity of $\delta^{34}S$ with other isotopes

Our results showed high complementarity of $\delta^{34}S$ with other isotopes on the individual and isoscape levels suggesting different environmental drivers of $\delta^{34}S$ and other isotopes. However, the high isoscape-level complementarity should be interpreted with caution. The feather samples used to predict the $\delta^{34}S$ isoscape in this study were formed in a single habitat type – wetlands. Wetland conditions likely differ from terrestrial conditions as indicated by the differences in geographic pattern of our isoscape and the European $\delta^{34}S$ isoscape from archaeological remains (Bataille et al. 2021). Our results show a high potential of $\delta^{34}S$ values in Europe, especially, in combination with other isotopes but a dense sampling of tissues from diverse taxa and across habitats is needed.

Conclusions

The predicted geographic distribution of $\delta^{34}S$ values in Europe shows high $\delta^{34}S$ values along the coastline in Europe and slight differences in $\delta^{34}S$ values between the central and southern parts of Europe. The absence of a systematic spatial pattern and high within-site variation limits the solitary use of the $\delta^{34}S$ isoscape. However, high levels of complementarity on the individual and isoscape levels suggest the potential of combining isoscapes to increase precision of animal tracing. Therefore, we encourage future studies to focus on geographic distribution of $\delta^{34}S$ in more homogeneous continents such as Africa, South America or East Asia. Moreover, we recommend to predict geographic distributions of $\delta^{34}S$ variables from samples collected in various environments, habitats, and from different animal species. We believe these efforts will significantly advance the

knowledge on the $\delta^{34}S$ geographic distributions and enhance their applications in ecological and forensics studies.

Acknowledgments

We are obliged to following bird ringers who helped us collect feathers samples in Europe: A. Leprêtre, A. Ożarowska, A. Trnka, A. Sponga, A. Pranaitis, B. Vollot, B. Fontaine, B. Bargain, C. Coleiro, R. Galea, C. Z. Martínez, C. Heroguel, C. Ion, D. Vigour, D. Dimitrov, M. Ilieva, D. Ragyov, D. Zhuravlev, D. Leoke, E. Baltag, F. G. Lopez, G. Goujon, J. R. Álvarez, J. Hlaváček, J. J. Baptiste, J. Kralj, J. Reif, J. Beier, J. M. Neto, K. and F. Breek, K. Bedev, K. Bairaktaridau, L. F. P. da Silva, M. Haluzík, M. Šćiban, M. Leconte, M. Olekšák, O. Zakala, P. S. Ranke, P. Matyjasiak, R. Thomas, R. Patapavičius, R. Slobodník, S. Gautier, S. Scebba, S. Capasso, S. Bräger, V. Cohez, V. Fedorov, V. Jusys, W. Fiedler, X. Commecy, Y. Beauvallet and Z. Karcza. We thank Gabriel Bowen and the Isotopes in Spatial Ecology and Biogeochemistry short course held at the University of Utah for providing the stimulating environment that led to this project. We are also thankful to Carol Kendall for initial advice and reviewers for their comments. Any use of trade, product, or firm names is for descriptive purposes only and does not imply endorsement by the U.S. Government.

Authors' contribution

VB conceived the idea of the study. VB, FJ, GO and PP collected or provided samples. LB and FC analysed stable isotopic composition of samples. VB designed the methodology with input from RLP, PP, CAS and MBW. VB conducted the analyses with input from MBW and RLP and took lead in the manuscript writing. All authors read, commented, and approved the final version of the manuscript.

Data accessibility

Sample metadata are stored and available for reuse in the AviSample Network database (https://avisample.net/: AS00001–AS00117)(Brlík et al. 2022a). The information on the isotopic composition and geographic origin of feather samples used to produce the $\delta^{34}S$ isoscape, predicted feather $\delta^{34}S$, $\delta^{2}H$ and $\delta^{13}C$ isoscapes are publicly available from the Zenodo data repository LINK (Brlík et al. 2022b).

Funding

This work was supported by the Grant Agency of Charles University (grant no. 254119), the National Science Foundation (grant no. DBI-1565128) and the Czech Science Foundation (grant no. 20-00648S).

Literature cited

Abatzoglou, J. T., Dobrowski, S. Z., Parks, S. A. and Hegewisch, K. C. 2018. TerraClimate, a high-resolution global dataset of monthly climate and climatic water balance from 1958–2015. - Sci. Data 5: 170191.

Amrani, A., Said-Ahmad, W., Shaked, Y. and Kiene, R. 2013. Sulfur isotope homogeneity of oceanic DMSP and DMS. - Proc. Natl. Acad. Sci. U. S. A. 110: 18413–18418.

Amundson, R., Austin, A. T., Schuur, E. A. G., Yoo, K., Matzek, V., Kendall, C., Uebersax, A., Brenner, D. and Baisden, W. T. 2003. Global patterns of the isotopic composition of soil and plant nitrogen. - Glob. Biogeochem. Cycles 17: 1031.

Bataille, C. P., von Holstein, I. C. C., Laffoon, J. E., Willmes, M., Liu, X.-M. and Davies, G. R. 2018. A bioavailable strontium isoscape for Western Europe: A machine learning approach. - PLoS One 13: e0197386.

Bataille, C. P., Crowley, B. E., Wooller, M. J. and Bowen, G. J. 2020. Advances in global bioavailable strontium isoscapes. - Palaeogeogr. Palaeoclimatol. Palaeoecol. 555: 109849.

Bataille, C. P., Jaouen, K., Milano, S., Trost, M., Steinbrenner, S., Crubézy, É. and Colleter, R. 2021. Triple sulfur-oxygen-strontium isotopes probabilistic geographic assignment of archaeological remains using a novel sulfur isoscape of western Europe. - PLoS One 16: e0250383.

Beck, H. E., Zimmermann, N. E., McVicar, T. R., Vergopolan, N., Berg, A. and Wood, E. F. 2018. Data Descriptor: Present and future Köppen-Geiger climate classification maps at 1-km resolution. - Sci. Data 5: 180214.

Belgiu, M. and Dragut, L. 2016. Random forest in remote sensing: A review of applications and future directions. - ISPRS J. Photogramm. Remote Sens. 114: 24–31.

Bowen, G. J. and Revenaugh, J. 2003. Interpolating the isotopic composition of modern meteoric precipitation. - Water Resour. Res. 39: 1–13.

Bowen, G. J., Liu, Z., Vander Zanden, H. B., Zhao, L. and Takahashi, G. 2014. Geographic assignment with stable isotopes in IsoMAP. - Methods Ecol. Evol. 5: 201–206.

Breiman, L. 2001. Random forests. - Mach. Learn. 45: 5–32.

Brlík, V., Pipek, P., Brandis, K., Chernetsov, N., Herrera M., L. G., Kiat, Y., Lanctot, R. B., Marra, P. P., Norris, D. R., Nwaogu, C. J., Quillfeldt, P., Saalfeld, S. T., Stricker, C. A., Thomson, R. L., Zhao, T. and Procházka, P. 2022a. The reuse of avian samples: opportunities, pitfalls, and a solution. - Ibis (Lond. 1859). 164: 343–349.

Brlík, V., Procházka, P., Bontempo, L., Camin, F., Jiguet, F., Osváth, G., Stricker, C., Wunder, M. and Powell, R. 2022b. Spatial distribution of feather sulphur isotopes in Europe. - Zenodo in press.

Buchhorn, M., Lesiv, M., Tsendbazar, N.-E., Herold, M., Bertels, L. and Smets, B. 2020. Copernicus Global Land Cover Layers — Collection 2. - Remote Sens. 12: 1044.

Case, J. W. and Krouse, H. R. 1980. Variations in Sulphur Content and Stable Sulphur Isotope Composition of Vegetation Near a SO2 Source at Fox Creek, Alberta, Canada. - Oecologia 257: 248–257.

Chambers, L. and Trudinger, P. 1979. Microbiological fractionation of stable sulfur isotopes: A review and critique. - Geomicrobiol. J. 1–3: 249–293.

Cherry, J. 2011. Ecology of Wetland Ecosystems: Water, Substrate, and Life. - Nat. Educ. Knowl. 3: 16.

CIESIN 2018. Gridded Population of the World, Version 4 (GPWv4): Population Density, Revision 11. Palisades, NY: NASA Socioeconomic Data and Applications Center (SEDAC). in press.

Copernicus Sentinel 2015a. Sentinel-5P NRTI SO2: Near Real-Time Sulphur Dioxide. in press.

Copernicus Sentinel 2015b. Sentinel-5P NRTI NO2: Near Real-Time Nitrogen Dioxide. in press.

Danielson, J. and Gesch, D. 2011. Global Multi-Resolution Terrain Elevation Data. - USGS Rep.: 1073.

Dansgaard, W. 1954. The O18-abundance in fresh water. - Geochim. Cosmochim. Acta1 6: 241–260.

Dansgaard, W. 1964. Stable isotopes in precipitation. - Tellus 16: 436–468.

Felicetti, L. A., Schwartz, C. C., Rye, R. O., Haroldson, M. A., Gunther, K. A., Phillips, D. L. and Robbins, C. T. 2003. Use of sulfur and nitrogen stable isotopes to determine the importance of whitebark pine nuts to Yellowstone grizzly bears. - Can. J. Zool. 81: 763–770.

Florin, S. T., Felicetti, L. A. and Robbins, C. T. 2011. The biological basis for understanding and predicting dietary-induced variation in nitrogen and sulphur isotope ratio discrimination. - Funct. Ecol. 25: 519–526.

Fry, B. 2006. Stable isotopes ecology. - Springer.

Garg, A., Shukla, P. R., Bhattacharya, S. and Dadhwal, V. K. 2001. Sub-region (district) and sector level SO2 and NOx emissions for India: assessment of inventories and mitigation flexibility. - Atmos. Environ. 35: 703–713.

Gorelick, N., Hancher, M., Dixon, M., Ilyushchenko, S., Thau, D. and Moore, R. 2017. Google Earth Engine: Planetary-scale geospatial analysis for everyone. - Remote Sens. Environ. 202: 18–27.

Grinkevich, V., Chernetsov, N. and Mukhin, A. 2009. Juvenile Reed Warblers Acrocephalus scirpaceus see the world but settle close to home. - Avian Ecol. Behav. 16: 3–10.

Hobson, K. A. and Wassenaar, L. I. 2018. Tracking Animal Migration with Stable Isotopes. - Academic Press.

Hobson, K. A., Van Wilgenburg, S. L., Wassenaar, L. I., Powell, R. L., Still, C. J. and Craine, J. M. 2012. A multi-isotope (δ13C, δ15N, δ2H) feather isoscape to assign Afrotropical migrant birds to origins. - Ecosphere 3: 44.

Jiguet, F., Robert, A., Lorrillière, R., Hobson, K. A., Kardynal, K. J., Arlettaz, R., Bairlein, F., Belik, V., Bernardy, P., Copete, J. L., Czajkowski, M. A., Dale, S., Dombrovski, V., Ducros, D., Efrat, R., Elts, J., Ferrand, Y., Marja, R., Minkevicius, S., Olsson, P., Pérez, M., Piha, M., Ranković, M., Schmaljohann, H., Seimola, T., Selstam, G., Sibblet, J.-P., Skierczyński, M., Sokolov, A., Sondell, J. and Moussy, C. 2019. Unravelling migration connectivity reveals unsustainable hunting of the declining ortolan bunting. - Sci. Adv. 5: eaau2642.

Kabalika, Z., Morrison, T. A., McGill, R. A. R., Munishi, L. K., Ekwem, D., Mahene, W. L., Lobora, A. L., Newton, J., Morales, J. M., Haydon, D. T. and Hopcraft, G. G. J. C. 2020. Tracking animal movements using biomarkers in tail hairs: a novel approach for animal geolocating from sulfur isoscapes. - Mov. Ecol. 8: 37.

Kuhn, M. 2008. Building predictive models in R using the caret package. - J. Stat. Softw. 28: 1–26.

Lott, C. A., Meehan, T. D. and Heath, J. A. 2003. Estimating the latitudinal origins of migratory birds using hydrogen and sulfur stable isotopes in feathers: Influence of marine prey base. - Oecologia 134: 505–510.

Martin, R. V, Jacob, D. J., Chance, K., Kurosu, T. P., Palmer, P. I. and Evans, M. J. 2003. Global inventory of nitrogen oxide emissions constrained by space-based observations of NO 2 columns. - J. Geophys. Res. 108: 4537.

McCutchan, J. H., Lewis, W. M., Kendall, C. and Mcgrath, C. C. 2003. Variation in trophic shift for

stable isotope ratios of carbon, nitrogen, and sulfur. - Oikos 2: 378–390.

Mukhin, A. 2004. Night movements of young Reed Warblers (Acrocephalus scipaceus) in summer: Is it postfledging dispersal? - Auk 121: 203–209.

NASA Ocean Biology Processing Group 2012. Distance to Nearest Coastline: 0.01-Degree Grid. in press.

Newton, J. 2021. An insect isoscape of UK and Ireland. - Rapid Commun. Mass Spectrom. 35: e9126.

Norris, D. R., Marra, P. P., Bowen, G. J., Ratcliffe, L. M., Royle, J. A. and Kyser, T. K. 2006. Migratory Connectivity of a Widely Distributed Songbird, the American Redstart (Setophaga ruticilla). - Ornithol. Monogr. 61: 14–28.

Ohizumi, T. and Fukuzaki, N. 1997. Sulphur isotopic view on the sources of sulphur in atmospheric fallout along the coast of the sea of Japan. - Atmos. Environ. 31: 1339–1348.

Pawlewicz, M. J., Williams, A. J., Walden, S. M. and Steinshouer, D. W. 2003. Generalized Geology of Europe including Turkey. - U.S. Geol. Surv. data release in press.

Popa-Lisseanu, A. G., Sörgel, K., Luckner, A., Wassenaar, L. I., Ibánez, C., Kramer-Schadt, S., Ciechanowski, M., Görföl, T., Niermann, I., Beuneux, G., Mysłajek, R. W., Juste, J., Fonderflick, J., Kelm, D. H. and Voigt, C. C. 2012. A triple-isotope approach to predict the breeding origins of european bats. - PLoS One 7: e30388.

Powell, R. L. and Still, C. J. 2010. Continental-Scale Distributions of Vegetation Stable Carbon Isotope Ratios. - In: West, J. B. et al. (eds), Isoscapes. Springer, pp. 495.

Powell, R. L., Yoo, E.-H. and Still, C. J. 2012. Vegetation and soil carbon-13 isoscapes for South America: integrating remote sensing and ecosystem isotope measurements. - Ecosphere 3: 1–25.

Powell, R., Firmin, S. and Griffith, D. 2019. grassmapr, an R package to predict C3/C4 grass distributions and model terrestrial δ13C isoscapes. in press.

Procházka, P., Van Wilgenburg, S. L., Neto, J. M., Yosef, R. and Hobson, K. A. 2013. Using stable hydrogen isotopes (δ2H) and ring recoveries to trace natal origins in a Eurasian passerine with a migratory divide. - J. Avian Biol. 44: 541–550.

Procházka, P., Brlík, V., Yohannes, E., Meister, B., Ilieva, M. and Hahn, S. 2018. Across a migratory divide: divergent migration directions and non-breeding grounds of Eurasian reed warblers revealed by geolocators and stable isotopes. - J. Avian Biol. 49: e01769.

R Core Team 2021. A Language and Environment for Statistical Computing. in press.

Rees, C., Jenkins, W. and Monster, J. 1978. The sulphur isotopic composition of ocean water sulphate. - Geochim. Cosmochim. Acta 42: 377–381.

Tcherkez, G. and Tea, I. 2013. 32S/34S isotope fractionation in plant sulphur metabolism. - New Phytol. 200: 44–53.

Thode, H. G. 1991. Sulphur isotopes in nature and the environment: an overview. - In: Stable isotopes: Natural and anthropogenic sulphur in the environment. pp. 1–26.

Thode, H. G., Macnamar, J. and Fleming, W. 1953. Sulphur isotope fractionation in nature and geological and biological time scales. - Geochim. Cosmochim. Acta 3: 235–243.

Troen, I. and Petersen, E. 1989. European Wind Atlas. - Riso National Laboratory.

Valenzuela, L. O., Chesson, L. A., O'Grady, S. P., Cerling, T. E. and Ehleringer, J. R. 2011. Spatial distributions of carbon, nitrogen and sulfur isotope ratios in human hair across the central United States. - Rapid Commun. Mass Spectrom. 25: 861–868.

Vapnik, V. N. 1998. Statistical Learning Theory. - Wiley.

Veen, T., Hjernquist, B., Van Wilgenburg, S. L., Hobson, K. A., Folmer, E., Font, L. and Klaassen, M. 2014. Identifying the African Wintering Grounds of Hybrid Flycatchers Using a Multi–Isotope (d2H, d13C, d15N) Assignment Approach. - PLoS One 9: e98075.

Villegas, M., Newsome, S. D. and Blake, J. G. 2016. Seasonal patterns in δ2H values of multiple tissues from Andean birds provide insights into elevational migration. - Ecol. Appl. 26: 2383–2389.

Wadleigh, M. A. and Blake, D. M. 1999. Tracing sources of atmospheric sulphur using epiphytic lichens. - Environ. Pollut. 106: 265–271.

West, J. B., Bowen, G. J., Dawson, T. E. and Tu, K. P. 2010. Isoscapes. - Springer.

Yu, Q., You, L., Wood-Sichra, U., Ru, Y., Joglekar, A. K. B., Fritz, S., Xiong, W., Lu, M., Wu, W. and Yang, P. 2020. A cultivated planet in 2010: 2. the global gridded agricultural production maps. - Earth Syst. Sci. Data: 1–40.

Zazzo, A., Monahan, F. J., Moloney, A. P., Green, S. and Schmidt, O. 2011. Sulphur isotopes in animal hair track distance to sea. - Rapid Commun. Mass Spectrom. 25: 2371–2378.